Investigation of the Water and Fuel Exposure Characteristics of Aircraft Fuel Tank Sealants and the Effect on their Glass Transition Temperature

S. Giannis,[1] R. D. Adams,[1] L. J. Clark,[2] M. A. Taylor[2]

[1]*Department of Mechanical Engineering, University of Bristol, Queen's Building, University Walk, Bristol BS8 1TR, United Kingdom*
[2]*Airbus, New Filton House, Filton, Bristol BS99 7AR, United Kingdom*

Received 16 July 2007; accepted 6 January 2008
DOI 10.1002/app.27961
Published online 27 February 2008 in Wiley InterScience (www.interscience.wiley.com).

ABSTRACT: The water and fuel absorption and desorption characteristics have been studied of aircraft fuel tank sealants. The sealants were an epoxy-cured polythioether and a MnO_2-cured polysulphide. The effect of the water and fuel exposure on the glass transition temperature was also investigated. Water diffusion was found to be Fickian for the polythioether sealant and the equilibrium plateau level was found not to be dependent on the immersion temperature. On the other hand, the polysulphide sealant demonstrated a clear non-Fickian water uptake characteristic, with large uptake levels, which were attributed to water droplet formation in the volume of the bulk sealant. The glass transition temperature of the polythioether sealant was not affected by the presence of water ($\sim$ 4% by weight) while that of the polysulphide was increased by $\sim$ 8°C for a water uptake level of $\sim$ 50% by weight. Fuel absorption followed a very similar trend for both sealants with the weight gain demonstrated an early maximum followed by a subsequent weight decrease, indicating leaching of fuel soluble fractions, until equilibrium was reached. The presence of fuel acted as plasticizer for the sealants; depressing their glass transition temperature by $\sim$ 10°C. Tests on dried samples have shown that the effect on the glass transition temperature was reversible. © 2008 Wiley Periodicals, Inc. J Appl Polym Sci 108: 3073–3091, 2008

Key words: sealants; polysulphide; polythioether; absorption; desorption; glass transition temperature; low temperature testing; dynamic mechanical analysis

INTRODUCTION

Nowadays, commercial aircraft are equipped with fuel tanks that are principally situated in their wings. These tanks, known as integral fuel tanks, are formed by the actual structure of the aircraft and contain large amounts of jet fuel. The use of integral fuel tanks is preferable in the aerospace industry since they utilize the primary structure, which is already designed to sustain loads. They demonstrate major advantages over rigid removable and bladder fuel tanks as they have a greater capacity and additionally they do not add more weight to the aircraft. However, the design of an integral fuel tank presumes the use of suitable materials that will provide and ensure a good seal of the structure throughout its service life. For such a sealant bond to be useful, it not only must withstand the mechanical forces that are acting on it, but it must also be resistant to elements to which it is exposed during service. Thus, one of the most important characteristics of a sealant joint is its endurance in the operating environment.

When immersed in liquids, sealants, like all polymers, experience diffusion of the molecules of the liquids into their volume. Within an aircraft fuel tank, hydrocarbons are the main constituents of the jet fuel, but there is an amount of water present due to atmospheric condensation. Consequently, aircraft fuel tank sealants are used in an environment where the presence of fuel and/or water could affect the bond as well as the bulk sealant. Potential failure of the sealant or the bond with the substrate may result in a fuel leak. In addition to fuel and/or water attack, fuel tank sealants operate over a wide temperature range. When in operation, an aircraft can experience temperatures down to −55°C. It becomes essential to know the behavior of the sealants after exposure to fuel and water, and how their performance is affected. When dealing with polymers, the glass transition temperature is an important property since it relates to significant changes in their behavior. The temperature at which an amorphous polymer experiences the transition from the rubbery to

Correspondence to: S. Giannis (sgiannis@merl-ltd.co.uk).
Contract grant sponsor: AIRBUS.

Journal of Applied Polymer Science, Vol. 108, 3073–3091 (2008)

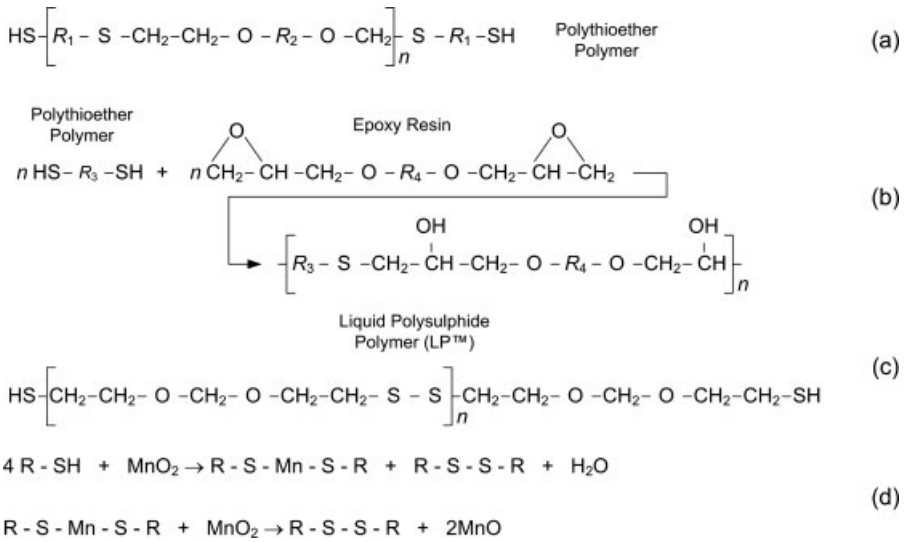

Figure 1 (a) Structure of polythioether polymer; (b) reaction of polythioether polymer with an epoxy resin; (c) structure of liquid polysulphide polymer (LP™); and (d) reaction of liquid polysulphide polymer with manganese dioxide.

the glassy state is termed as the glass transition temperature (T_g). The presence of flexible molecular groups in the polymer backbone, the polarity of the polymer backbone, the molecular weight, the cross-link density, the addition of plasticizers, and the environment are some of the factors that affect the glass transition temperature of a polymer.

Only few data are available in the literature concerning the effect of the environment on the behavior of sealants and sealant joints,[1–3] although there is much on the durability of structural adhesives.[4–6] Gick[1] studied extensively the diffusion of aviation fuel and water in polysulphide sealants and concluded that, for immersion in aviation fuel (Avtur), the mass uptake behavior was explicable by Fickian diffusion while anomalous non-Fickian diffusion was observed during immersion in water. The amount of water absorbed was found to be strongly dependent on the amount and nature of the curing agent residues in the sealant material. Comyn et al.[3] also studied the diffusion of water, aviation fuel, and antifreeze in a number of sealants and the effect on the durability of joints. They demonstrated that the best guide to assess the durability of sealant joints was the amount of liquid absorbed by the sealant.

In the present work, we investigated the behavior of two aircraft fuel tank sealants when these are immersed in water and jet fuel. The diffusion behavior of the sealants was assessed through liquid absorption and desorption tests. The effect of the water and fuel absorption on the glass transition temperature of the sealants was also investigated and the results were discussed based on physical and chemical considerations.

MATERIALS

Sealant materials

The aircraft fuel tank sealants tested here are named Sealant A and Sealant B. The trade names of the two sealants are omitted since both are commercially available, and the present study is not, by any means, a comparative work between commercial products. Both sealants are used for interfay as well as fillet sealing of integral fuel tanks and other aircraft fuselage sealing applications.

Sealant A is a two-part epoxy cured polythioether polymer with a service temperature range from −55°C to +160°C. The structure of the epoxy-cured polythioether sealant and the cure reaction with a conventional epoxy are shown in Figure 1(a,b). The chemistry of the polythioether-based sealants has been discussed in the literature.[7]

Sealant B is a two-part manganese dioxide (MnO_2) cured, liquid polysulphide polymer (LP™) with a service temperature range from −55°C to +130°C. LP polymers, which have been the basis of the aerospace sealant industry for over 40 years, are produced by the aqueous polymerization of bis(2-chloroethyl)-formal with sodium polysulphide.[8] The result is a linear polymer terminated with mercaptan groups (—SH), as shown in Figure 1(c). The mercaptan terminated LP™ monomer is polymerized using oxidizing agents to formulate the final elastomeric sealant product.[9] Sealant B uses manganese dioxide (MnO_2) as the curing agent. The cure mechanism that leads to the formation of the final elastomeric sealant product, as summarized by several researchers (for e.g., Refs. 8,9), can be seen in Figure 1(d).

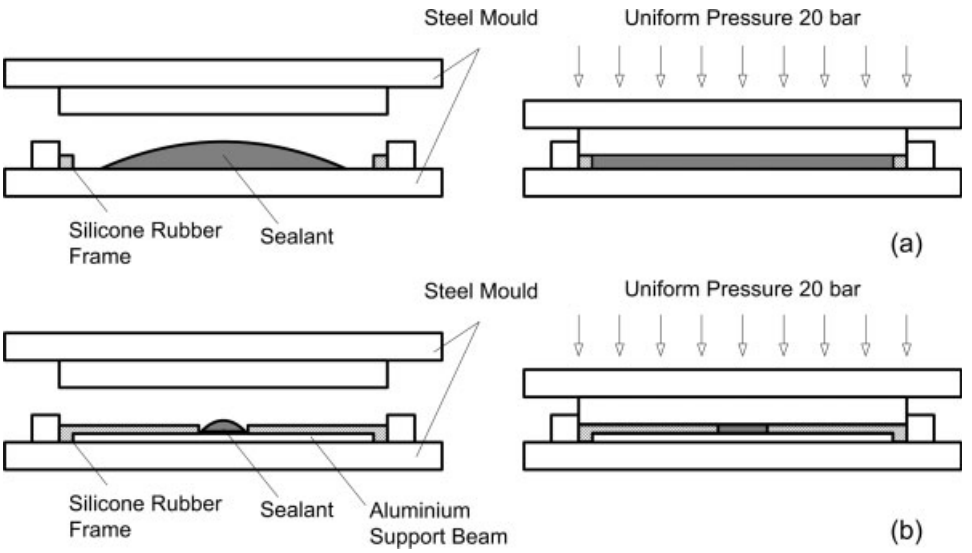

Figure 2 Schematic representation of the manufacturing technique with hydrostatic pressure used to produce (a) uniform sheets of bulk sealants and (b) specimens for T_g evaluation.

Commercial aircraft fuel tank sealants also contain a number of compounds such as cure modifiers, fillers (e.g., calcium carbonate), plasticizers and adhesion promoters. All these compounds play a significant role in the properties of the cured elastomeric sealant.

EXPERIMENTAL

Preparation of specimens for water/fuel uptake measurements

Water and fuel mass uptake experiments were performed on bulk Sealant A and Sealant B samples. To produce thin sheets of bulk sealants, a hydrostatic pressure technique was adopted as described in the French standard NFT 76-142[10] and extensively used[11] to produce bulk adhesive sheets of uniform thickness without porosity. The technique consists of curing flat sheets of adhesive and/or sealant in a metallic mold, sealed with a silicon rubber frame, under hydrostatic pressure (20 bars). The components (base and curing agent) of the two sealants were mixed in a ratio 10 : 1 by weight. A specific amount of mixed sealant, slightly greater than the volume corresponding to the internal part of the silicone rubber frame, was then poured into the middle of the mold [Fig. 2(a)]. At that stage, a gap was left deliberately between the freshly mixed sealant and the silicone rubber frame; at the moment of the application of the pressure, this enabled the sealant to flow until the mold was completely filled and, in this way, air entrapment in the middle of the mold could be avoided. An external metallic frame was used to keep the silicone rubber frame in place. Both sealants were initially left to cure under hydrostatic pressure for 24 h at room temperature (23°C ± 2°C and 55% ± 5% RH). After that, the pressure was released and the mold was placed in an oven for the next 24 h at 50°C (35% RH). The dimensions of the sealant material sheet after cure were ~ 200 mm × 60 mm, with a nominal thickness of 0.85 mm, which corresponds to the dimensions of the silicone rubber frame used to produce the hydrostatic pressure.

Water/fuel uptake measurements

To measure the diffusion behavior of the aircraft fuel tank sealants, samples of each sealant, having nominal dimensions 40 mm × 15 mm × 0.85 mm, were cut from the cured sheets. The thickness of the samples was made small compared to its width and length; the ratio of the edge surface area to the total surface area was ~ 7%, such that edge effects could be ignored and the diffusion could be regarded as being one-dimensional. All the samples were conditioned at 50°C for 0.5 h under vacuum to ensure that moisture preexisting in the sample would be removed prior to immersion. Samples were then immersed either in distilled water or in Type III synthetic jet fuel which is a synthetic test fluid composed of a blend of Iso-Octane (70% by volume) and Toluene (30% by volume).[12] For the case of water immersion at elevated temperatures, specimens were placed in distilled water chambers maintained at constant temperatures of 40 and 50°C. For the case of water and fuel immersion at ambient temperature, samples were placed in sealed glass jars, containing distilled water or fuel. In all cases, the temperature was monitored via a digital thermometer. The specimens were periodically removed from their environment, weighed, and returned to the baths. To ensure the removal of excessive surface liquid, before

weighing, specimens were gently wiped dry using clean, lint-free tissue paper. Weight measurements were taken using an electronic analytical balance (METTLER PM2500 Delta Range®) measuring to 0.1 mg.

The percentage mass increase M_t at time t was calculated using the following relationship:

$$M_t = \frac{m_t - m_0}{m_0} \times 100\% \quad (1)$$

where, m_t, m_0 are the mass of the specimen after an immersion period of time t, and before immersion, respectively.

After exposure to distilled water or jet fuel for a given period of time, all the specimens, even those that had not reached equilibrium, were placed in a controlled chamber to desorb liquid from the surface of the specimens. The temperature was set to the temperature of the immersion process. For the case of specimens immersed in water or fuel at ambient temperature, the desorption process also took place at room temperature. During the desorption process, specimens were weighed regularly to determine the percentage weight change.

Preparation of specimens for T_g measurements

For the evaluation of the glass transition temperature, an in-house DMA (dynamic mechanical analysis) testing method was used. This method involves a sealant layer cured on top of a metallic beam. Flexural vibration of this composite beam can be used to evaluate the glass transition temperature of the sealant layer. The variation of the resonance frequency of a homogeneous metallic beam and the same beam with a uniform sealant layer on top, vibrating in the free–free flexural mode at the first resonant frequency, is shown in Figure 3. The resonance frequency is proportional to the square root of the modulus of the material. As a result, at low temperatures, the resonance frequency of the metallic beam is high, due to the high stiffness of the material and it decreases as the temperature increases. Because the metallic beam does not experience any transition, the variation of the resonance frequency, and consequently the modulus, for the given beam is uniform with respect to the temperature. If a uniform layer of sealant is added on top of the same metallic beam then the resonance frequency of the composite beam (support + sealant layer) will change. What will actually happen is that at very low temperatures, due to the additional stiffness of the sealant layer, the resonance frequency of the composite beam will be higher than that of the metallic beam alone. As the temperature increases, the sealant material passes through the glass transition temperature and the stiffness of the overall beam decreases dramatically. Consequently, the resonance frequency decreases. At higher temperatures, the stiffness of the sealant is very low and the sealant layer only adds mass to the composite beam, so the resonance frequency is lower than that of the metallic beam alone. Thus, from the variation of the resonance frequency of such a composite beam, a glass transition temperature can be measured, as the temperature in the middle of the transition region. In a similar way, a glass transition temperature can be obtained from the variation of the damping of the same composite beam with respect to the temperature, since it demonstrates a maximum value that can be used as a measure of T_g.

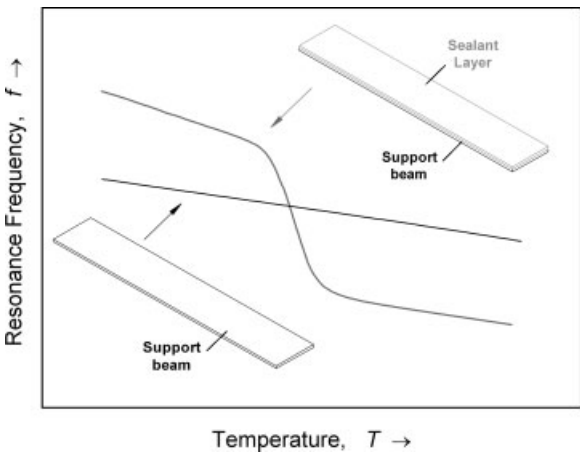

Figure 3 Schematic variation of the resonance frequency with respect to the temperature for a homogeneous metallic beam and the same beam with a uniform layer of sealant on top.

For measuring the glass transition temperature of the sealant materials, an aluminum alloy beam, having nominal dimensions 150 mm × 25 mm × 1.6 mm, was used as the support beam. It was found experimentally that when the overall length of the support beam was covered with a uniform layer of sealant, the damping of the composite system was very high, especially close to the glass transition temperature, and the amplitude of the vibration was very small and difficult to measure. T_g specimens were therefore manufactured by curing a small layer of sealant at the middle of the support beam, as shown in Figure 4(a). No surface treatment was applied to the aluminum prior to the application of the sealant since the degree of adhesion with the sealant layer was sufficient. The same manufacturing technique as for the bulk sealant sheets was used to apply the sealant to the top of the aluminum beams [Fig. 2(b)]. The beams were placed in a sealed metallic mold and the required amount of the mixed sealant was poured on top of them. A silicone rubber frame was responsible for restricting the sealant only

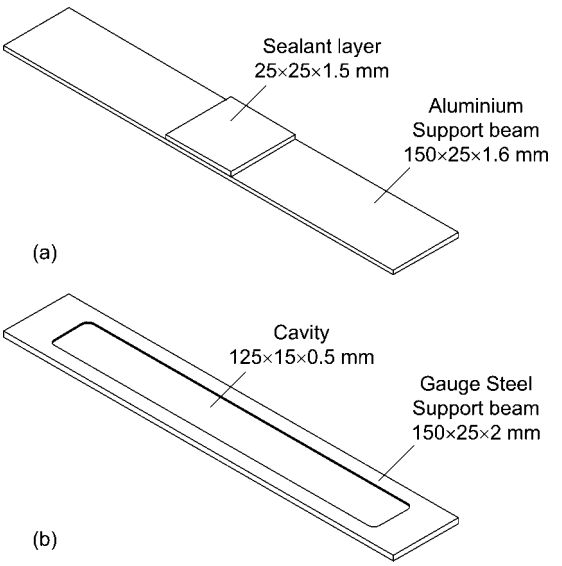

Figure 4 (a) Beam specimens used for the evaluation of T_g of cured sealants and (b) support beam used for the evaluation of that of the uncured sealant components.

to the middle part of the beam. In addition, the frame determined the final thickness of the cured sealant layer, which was set to 1.5 mm. The pressure applied to the sealed mold was 20 bar and the curing profile was the same as for the bulk sealant sheets.

Testing the uncured sealant components (base and curing agent) using the same technique was more difficult because of their low viscosity. Producing a layer of these materials was impossible, so it was decided to machine a cavity on a gauge steel beam and to pour the liquid polymer into the cavity [Fig. 4(b)]. In that way, a layer of the liquid was cast on the beam although it did not cover the whole area. By testing this composite beam, it was found that the amount of polymer was enough to damp the system and so to enable the glass transition temperature to be measured.

T_g measurements

A resonant beam technique was used for monitoring the vibrational behavior of composite beams over a wide temperature range and allow for the evaluation of the glass transition temperature of the sealants under investigation. This method does not require an accurate measurement of the excitation force or the response displacement. All that is needed is to vibrate the composite beam in a known resonant mode of vibration, then to record both the resonance frequency and the damping with respect to the temperature. Details of the experimental setup used to produce the flexural vibrations and monitor the resonance frequency can be found elsewhere.[13,14]

The most important parameter to be measured is the temperature of the material during testing. The use of a thermocouple directly connected on the vibrating specimen is not recommended, because it will affect both the natural frequency and the damping of the system. It was therefore decided that a dummy specimen, placed next to the vibrating specimen, should be used to monitor the temperature of the sealant. The dummy specimen was similar in dimensions to the vibrating specimen and when the test was performed after exposure in fuel or water it had also been exposed for the same amount of time. The dummy specimen carried an embedded thermocouple, which was connected to a personal computer. The temperature of the dummy specimen was measured at the same time intervals as the resonance frequency and damping of the vibrating specimen. The temperature was measured in both the cooling and warming stages of the test as can be seen in Figure 5. The cooling rate was very fast because of the fixed liquid nitrogen feed rate in the environmental chamber. On the other hand, during warming there was no energy input to the system, which was allowed to warm up only by the heat exchange of the chamber with the external environment. Consequently, the warming rate was very slow and varied with time.

By plotting the variation of the recorded resonance frequency and damping, as given by the inverse of the amplitude of the vibration, with respect to the temperature, the glass transition temperature was evaluated. Tests for T_g were performed on a number of specimens, initially conditioned at 50°C for 0.5 h under vacuum. After the DMA tests, some of the specimens were placed in distilled water baths at 50°C and some in sealed glass jars containing synthetic fuel at 25°C. The glass transition temperature was reevaluated when the specimens reached their

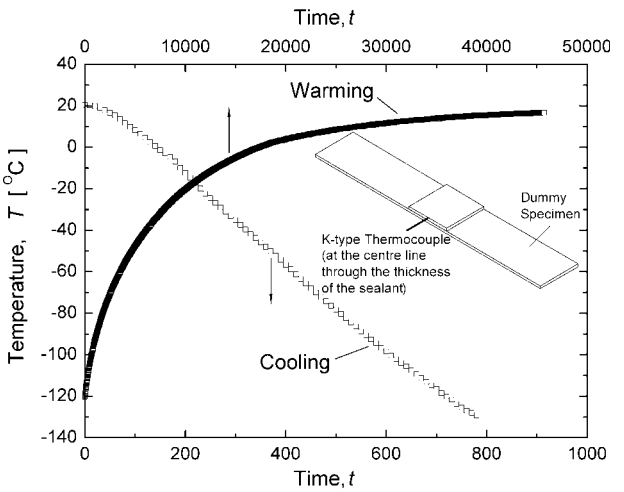

Figure 5 Variation of temperature with respect to the time as measured using a dummy specimen during the cooling and warming stages of the dynamic mechanical tests.

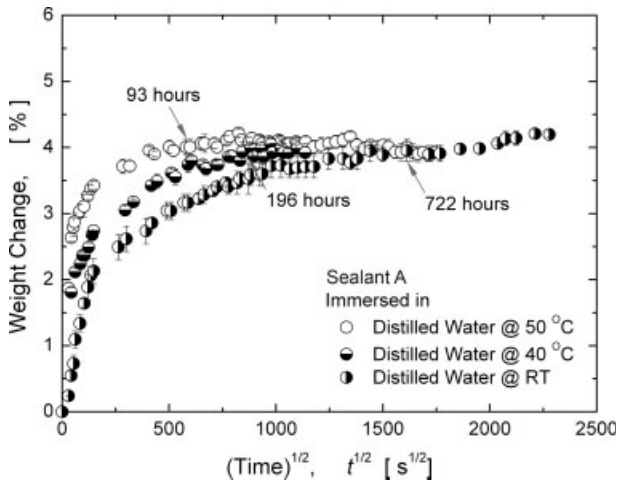

Figure 6 Percentage weight change data plotted with respect to the square root of time for Sealant A samples immersed in distilled water at different temperatures.

saturation level. Finally, the saturated samples were dried at the same temperature as the immersion temperature and the glass transition temperature was measured again after the end of that process. This could give an indication of whether any changes in T_g, because of the presence of water or fuel, were reversible or not.

RESULTS AND DISCUSSION ON WATER AND FUEL EXPOSURE TESTS

For Fickian diffusion, the weight gain of the immersed samples is given by:[15]

$$M_t/M_\infty = 1 - \sum_{n=0}^{\infty} \left[8\pi^2(2n+1)^2\right] \times \exp\left[-D(2n+1)^2\pi^2 t/h^2\right] \quad (2)$$

where, M_t is the weight attained at time t, M_∞ is the weight attained at equilibrium, D is the diffusion coefficient, and h is the thickness of the sample. In such a case, the two parameters that fully describe the diffusion process are the following: the diffusion coefficient, D, which is a measure of the ease with which a penetrant molecule can travel in a polymer, and the equilibrium level, M_∞. For short immersion times eq. (2) can be rewritten as:

$$M_t/M_\infty = 4(Dt/\pi)^{1/2}/h \quad (3)$$

Equation (3) implies that if the weight gain is plotted with respect to the square root of immersion time, then the initial part of the plot (short immersion times) is a straight line passing through the origin and of slope $4(D/\pi)^{1/2}h$. If the locus then leads to an equilibrium plateau the system is showing Fickian diffusion.[16] Therefore, from the experimental weight gain data, the diffusion coefficient calculation is enabled by considering the slope of the initial linear part of the curve and the level attained at equilibrium.

Water absorption and desorption

The weight change of Sealant A samples immersed in distilled water at three distinct temperatures is plotted in Figure 6 as a function of the square root of time of immersion. Each data point is the average value of five individual samples weighed separately. The results clearly show that the immersion temperature does not significantly affect the moisture level attained at equilibrium, which was found to be 4.17%, 3.95%, and 4.06% for samples immersed at room temperature (23°C ± 2°C), 40°C, and 50°C, respectively. On the other hand, the rate of diffusion appears to be noticeably affected. The diffusion of water into Sealant A can be described as Fickian with respect to the weight change, which shows an initial linear part followed by a transition region, reaching an equilibrium plateau after 722, 196, and 93 h, for 23, 40, and 50°C, respectively. Following the immersion process, all the samples that were immersed in distilled water at 40 and 50°C were dried in a chamber (35% RH) previously set to a temperature equal to the immersion temperature. Figure 7 shows the variation of the weight change as a function of $t^{1/2}$ during the drying process. The weight change data is reported with respect to the initial weight of the dry samples. For both temperatures, the sealant samples lost the gained weight rapidly and they reached mass equilibrium at a level less than their initial mass (−2.14% for drying at

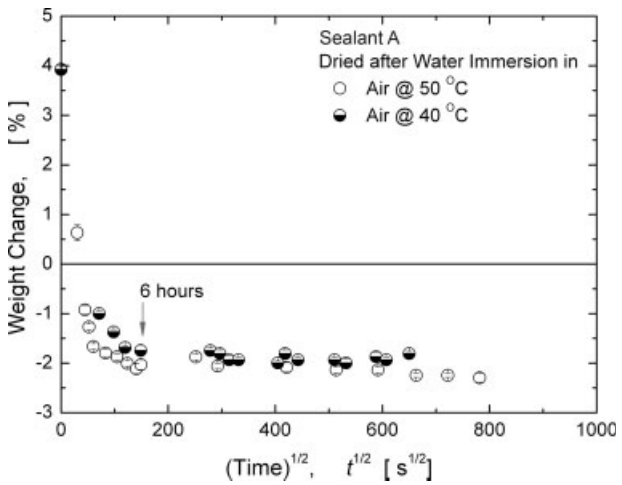

Figure 7 Percentage weight change data plotted with respect to the square root of time for Sealant A samples during desorption.

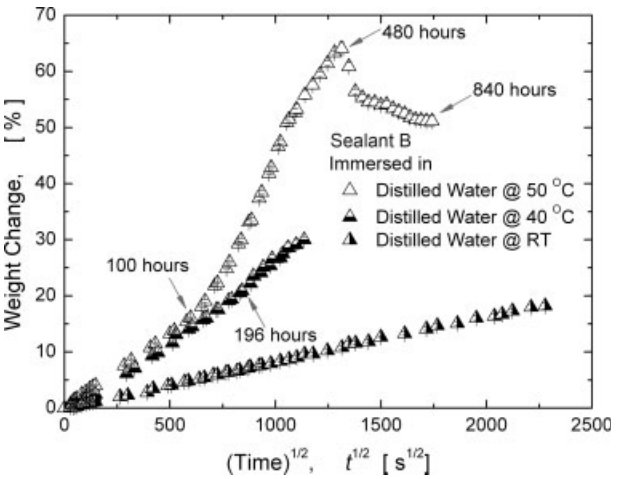

Figure 8 Percentage weight change data plotted with respect to the square root of time for Sealant B samples immersed in distilled water at different temperatures.

50°C and −1.89% for drying at 40°C), after ∼ 6 h. The negative values indicate leaching of constituents, possibly some unreacted sealant components and/or small molecular weight components. Strong evidence of material leaching out was the decolorization of the distilled water after the end of the immersion process and the fact that there was an apparent change in color of the samples, which turned from dark gray to light gray.

Figure 8 shows the variation of the weight change as a function of $t^{1/2}$ for Sealant B. Unlike Sealant A, Sealant B shows clear non-Fickian diffusion behavior, which is also strongly dependant on the immersion temperature. When immersed in distilled water at 40°C, Sealant B initially exhibited a linear water uptake with respect to $t^{1/2}$ and, after 196 h, the weight gain rate seemed to increase slightly. However, the immersion period was restricted to 360 h for these preliminary tests, so there were no clear signs of the likely overall behavior of the examined material. A set of samples was immersed in distilled water at room temperature and the diffusion process was found to be very slow while the weight gain increased continuously with $t^{1/2}$. Water immersion was also performed at 50°C, as illustrated in Figure 8. In this case, during early immersion in the distilled water (∼ 100 h), the weight gain increased linearly with $t^{1/2}$. Then, the weight gain rate increased significantly and, during the final stages of the immersion process (last 360 h), there was some weight loss. After 840 h of immersion, the amount of weight gain was found to be 51.90%. An analogous behavior while testing a similar material system was observed previously by Usmani et al.[17] In that case a manganese dioxide-cured polysulphide sealant was immersed in water at 60°C and it was found that the weight gain increased linearly with $t^{1/2}$ over the first 300 h, reaching a value of ∼ 20%. After that, the moisture absorption rate became higher and there was noticeable swelling of the material. The observed behavior was attributed to chemical stress relaxation that could promote the high water gain. Anomalous moisture uptake was recently reported by Loh et al.[18] in the investigation of a rubber toughened epoxy adhesive at various levels of relative humidity. They successfully modeled the moisture uptake process using a dual stage diffusion model.

The water immersion process of Sealant B samples was followed by subsequent drying in a chamber set to the same temperature as the immersion temperature (Fig. 9). All the samples showed a relatively quick weight loss and the mass equilibrium level after 168 h at 50°C was −2.43%, while for the specimens dried at 40°C for 120 h it was −1.94%. In other words, the samples immersed in distilled water at 50°C and then dried at the same temperature showed 25% higher final weight reduction than these immersed and dried at 40°C. This difference is believed to be mainly due to the different duration of the immersion process that led to additional leaching for the samples immersed at 50°C. Leaching of material constituents was again evident from the color of the distilled water after the end of the immersion process.

ESEM (environmental scanning electron microscopy) micrographs presented in Figure 10 shows that the through-thickness morphology of Sealant B is affected significantly by the water immersion. Dry and water immersed samples were sectioned and images were taken. What appears to be a homogeneous material before the water immersion, seems to possess a spongy structure after long term exposure in water. This, of course, could be strongly related to leaching of material constituents during the immer-

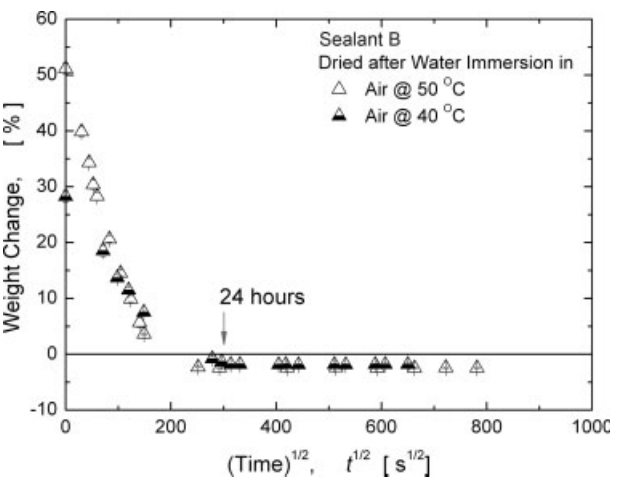

Figure 9 Percentage weight change data plotted with respect to the square root of time for Sealant B samples during desorption.

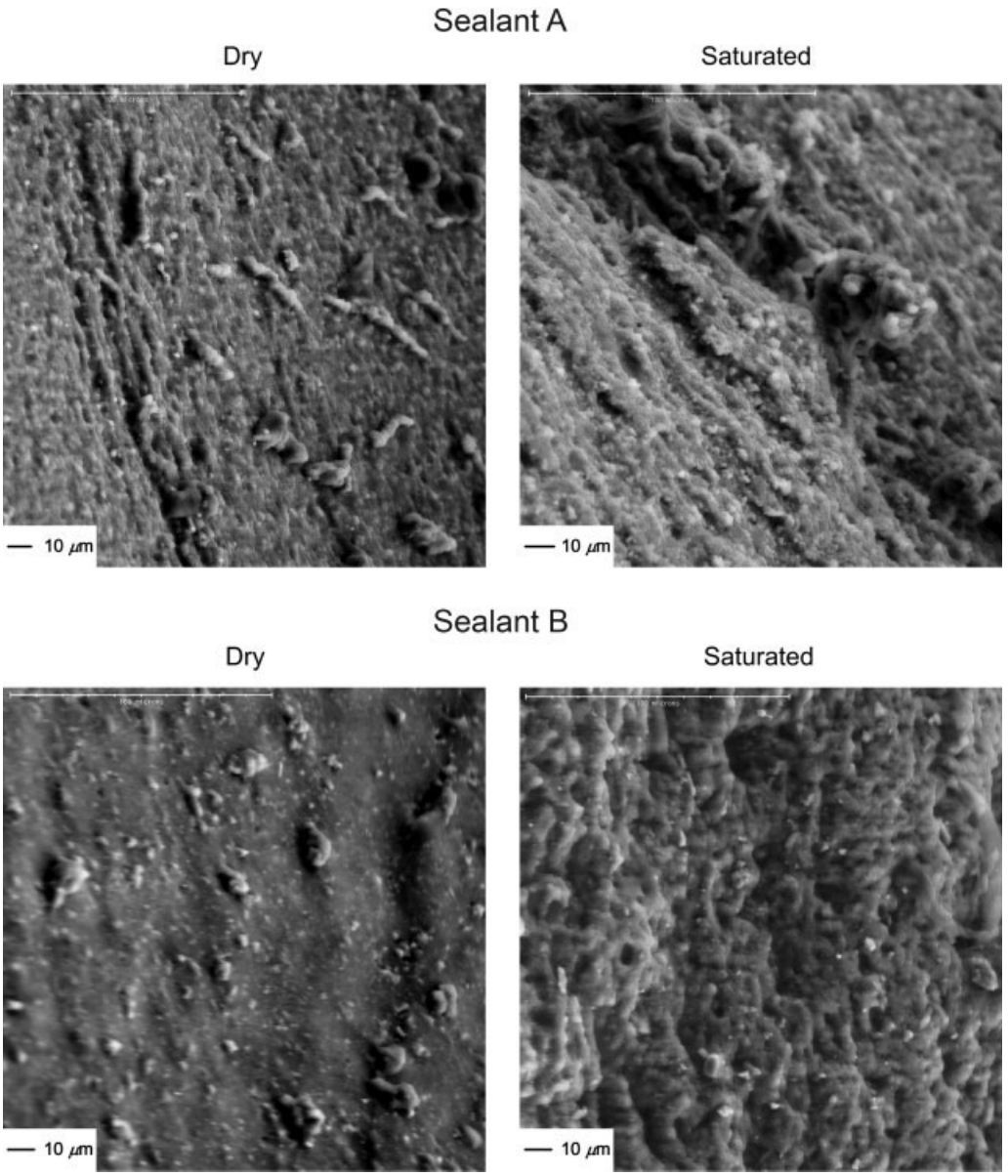

Figure 10 ESEM micrographs of Sealant A and Sealant B dry and wet samples after long term immersion in distilled water (magnification ×500).

sion process. No significant changes in the morphology of Sealant A were found before and after immersion in distilled water (Fig. 10).

Water absorption mechanisms

The experimental results undoubtedly indicate that Sealant A demonstrates Fickian water diffusion. The mechanisms of such a type of diffusion are comprehensively presented elsewhere.[16] On the other hand, Sealant B clearly demonstrates abnormal, non-Fickian, water diffusion. This abnormal behavior can be attributed to the formation of water droplets in the bulk of the material. The idea of water droplet formation in elastomeric materials during the diffusion of water is not new and it is based on considerations of water soluble impurities existing within the materials. Elastomers usually contain hydrophilic impurities. In addition, vulcanizing agents, fillers, and compounding ingredients can also lead to hydrophilic materials being present within the elastomer. The mechanism of diffusion of water, as summarized by Gick,[1] is based on two assumptions: (a) that the impurities are present in particulate form and are uniformly dispersed all over the elastomer and (b) a small proportion of water is in true solution in the elastomeric material. When an elastomeric material is immersed in water, the water is transported in the elastomer after a concentration gradient is established. However, when reaching the hydrophilic

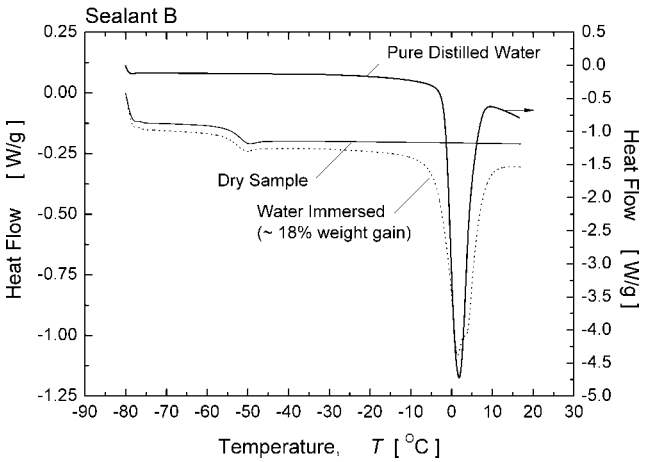

Figure 11 DSC plots of dry and wet Sealant B samples (the DSC curve of pure distilled water is also plotted for comparison).

impurities, the water concentrates to form droplets of solution. The droplets act as sinks which reduce the rate of diffusion but increase the amount of water in the elastomer. This mechanism implies that there is a nonuniform water distribution throughout the elastomer prior to equilibrium. The material close to the droplets is at a greater stress level compared with regions of elastomer that do not contain any droplets. Once a true solution of water and hydrophilic impurities is created, water will continue to enter the droplet of solution until there is a balance between the elastic forces resisting expansion of the droplet and the osmotic forces tending to expand the droplet. The osmotic forces result from the difference in osmotic pressure between the external solution and the droplet solution within the elastomer and it is these that govern the diffusion in the whole of the elastomeric material.[19]

Evidence for existence of such droplets of water in Sealant B samples was obtained by DSC tests using a Q100 TA Instruments DSC with a heating rate of 10°C/min. The results obtained both before and after water immersion are presented in Figure 11 where it can be seen that the DSC plot of the water-immersed samples demonstrates a melting peak which correlates well with the melting peak of the pure distilled water. However, in the sealant, the water droplets do not contain pure water but a solution of water and water soluble impurities. For this reason, there was a depression of the temperature corresponding to the peak of the immersed samples compared with that of the pure distilled water by 0.4°C. It is, therefore possible that some of the water absorbed by Sealant B forms ice during the cooling stage that then melts during warming. On the other hand, no such effect was observed when DSC runs were performed for Sealant A samples both before and after water immersion. This indicates that while the water diffuses into the bulk material, it does not form droplets.

In a previous study[20] where the high temperature absorption of water for a range of elastomeric materials was investigated, the effects of impurities on water uptake were quantified by using cryogenic techniques. The existence of water present in droplets was proved and an estimation of the droplet size was made (spherical shape $\sim$ 3 μm in diameter) from the depression of the water freezing point. Comyn et al.[3] have also attributed the high water uptake levels of a chromate-cured polysulphide sealant to the formation of droplets, possible slow hydrolysis, and/or build up of water at the sealant-filler interface. The weight gain curve for Sealant B immersed at 50°C was found to have a sigmoidal shape, which fits well with data reported by others for manganese dioxide-cured as well as calcium dichromate-cured sealants.[1] In that particular work, the larger water uptake by the calcium dichromate-cured sealant was credited to the higher solubility of calcium dichromate in water. It was also pointed that if exclusively organic curing agents were used, then the water uptake was the lowest. Apart from the high water uptake, it was also noticed that there was a significant volumetric swell of the Sealant B samples ($\sim$ 69%). Comparable values can be found in the literature,[21] where the volume swell of manganese dioxide-cured polysulphide sealants after water immersion was studied and it was reported that the volume swell was in the range of 40–60% after 840 h of immersion in water at 50°C. Finally, in another work,[22] the inferiority of manganese dioxide-cured sealants against dichromate-cured sealants to resist swelling due to autoxidation processes that take place in the bulk of the material when immersed in hot water was demonstrated.

Fuel absorption and desorption results

Fuel absorption characteristics were also examined by mass uptake experiments on initially dry Sealant A samples, immersed in Type III jet fuel at room temperature. It was found that Sealant A initially absorbs fuel rapidly up to a level of 7.65%. It therefore seems that a leaching effect became more significant and the weight of the samples decreased until it finally stabilized at a level of 6.60%, after 236 h [Fig. 12(a)]. Following immersion in fuel, the samples were placed in a chamber set at room temperature to dry out. Figure 12(a) also shows the variation of the weight change as a function of $t^{1/2}$, for this drying process. The samples lost their gained weight fairly quickly and they reached an equilibrium level of -1.97%, in a period of 50 h. This negative value corresponds to the total leaching of constituents during the immersion stage for Sealant A. The behavior

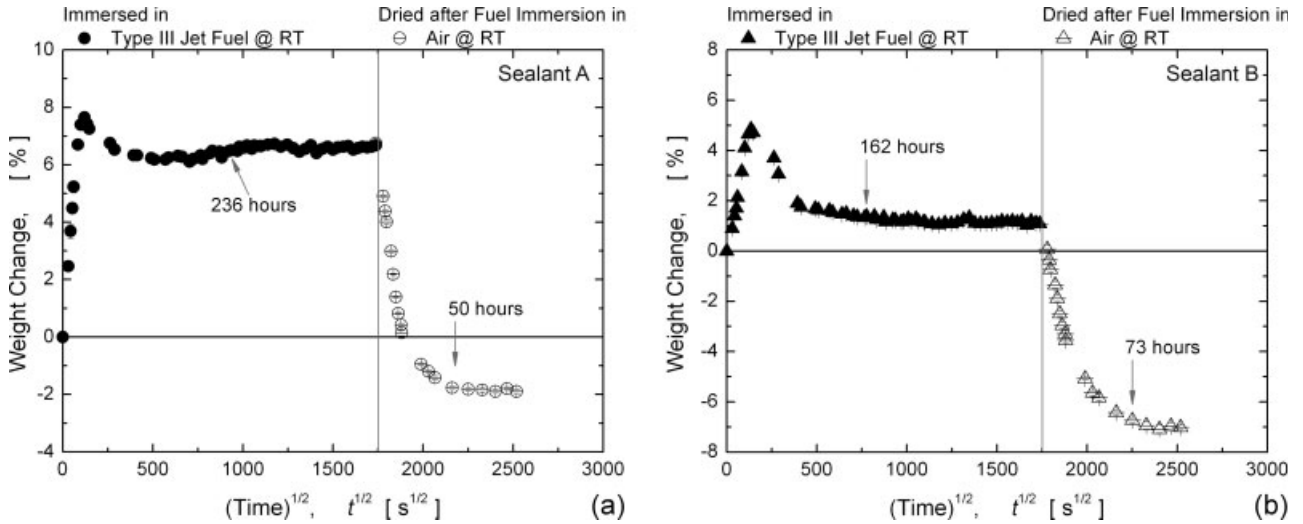

Figure 12 Percentage weight change data plotted with respect to the square root of time for (a) Sealant A and (b) Sealant B samples during jet fuel absorption and desorption.

of Sealant B samples immersed in Type III jet fuel [Fig. 12(b)] was very similar to that of Sealant A, with an initially rapid increase up to a level of 4.84%, followed by a period where significant leaching occurs and, finally, the weight change stabilizes at a level of 1.16% after 162 h. The level at equilibrium for Sealant B (1.16%) was much lower than 7%, a value obtained in another work[17] for a manganese dioxide-cured polysulphide sealant immersed in jet reference fuel at 60°C. However, it fits quite well with the observations by other researchers,[3] where it was also noticed that there was an early maximum in the weight gain curve followed by a decrease in weight, until equilibrium was reached at a level of about 1.1%, for a chromate-cured polysulfide sealant in aviation fuel. During the drying process that followed the immersion process [Fig. 12(b)], the samples lost their gained weight fairly quickly and they reached an equilibrium level of −7.02%, after 73 h. As for Sealant A, the equilibrium level after the drying process corresponded to the total leaching of material constituents.

Diffusion coefficients

The diffusion coefficient for all cases (absorption and desorption) was calculated and is listed in Table I. Unbracketted values of M_∞ are final equilibrium values, but brackets indicate that equilibrium had not been attained and that the values given are those at the termination of the tests. It is the values of M_∞^* that were used for the calculation of the diffusion coefficient as they are the most appropriate, since there was significant leaching during the fluid uptake tests and the final level at equilibrium, M_∞, does not directly give the mass of water or fuel absorbed by the samples.

TABLE I
Absorption and Desorption Characteristics of Sealant A and Sealant B in Water and Fuel

Material	Test	M_∞ (%)	M_∞^* (%)	$D \times 10^{-12}$ (m^2/s)
Sealant A	Immersed in water at 50°C	4.06	6.20	13.3
	Immersed in water at 40°C	3.95	5.84	5.5
	Immersed in water at RT	4.17	4.17	1.8
	Dried in air at 50°C	−2.14	−6.20	39.4
	Dried in air at 40°C	−1.89	−5.84	12.7
	Immersed in jet fuel at RT	6.60	8.57	13.8
	Dried in air at RT	−1.97	−8.57	4.3
Sealant B	Immersed in water at 50°C	51.90	54.33	0.035
	Immersed in water at 40°C	(30.02)	31.96	0.027
	Immersed in water at RT	(18.22)	18.22	0.021
	Dried in air at 50°C	−2.43	−54.33	6.9
	Dried in air at 40°C	−1.94	−31.96	2.7
	Immersed in jet fuel at RT	1.16	8.18	2.6
	Dried in air at RT	−7.02	−8.18	2.0

TABLE II
Diffusion Coefficients of Sealants Immersed in Jet Fuel

Material	Test	$D \times 10^{-12}$ (m^2/s)	Source
Sealant A (epoxy-cured polythioether)	Type III jet fuel at RT (23°C ± 2°C)	13.8	Present work
Sealant B (MnO_2-cured polysulphide)		2.6	
$CaCr_2O_7$-cured polysulphide	Aviation fuel at 25°C	0.9	Gick[1]
Chromate-cured polysulfide		1.39	Comyn et al.[3]
Fluorosilicone		13	
Butadiene-acrylonitrile-epoxide		1.5	Comyn et al.[24]

The diffusion coefficient for Sealant A immersed in distilled water was of the order of 10^{-12} m^2/s for all three temperatures. It was also found to increase considerably with temperature, signifying that water molecules diffuse into the sealant volume easier at higher immersion temperatures (thermally activated process). During desorption, D was once more found to increase with temperature. Moreover, for the same temperature (e.g., 50°C) the desorption diffusion coefficient was significantly higher than that during absorption (39.4×10^{-12} m^2/s compared to 13.3×10^{-12} m^2/s). This implies that the time required for the loss of a given amount of water from a saturated sample is less than that required for the absorption of the same amount by a dry sample. The reason for this is the particular dependence of the diffusion coefficient with concentration. In fact, the diffusion coefficient decreases with increasing water concentration.[15,19]

For Sealant B, an estimate of the diffusion coefficient was made, although there was no end to the saturation process for the immersion at room temperature and at 40°C, and the immersion at 50°C was clearly non-Fickian. The values found were of the order of 10^{-14} m^2/s, which compares well with values reported elsewhere.[3,23] The diffusion coefficient during desorption of Sealant B samples was found to be much higher (of the order of 10^{-12} m^2/s).

Diffusion coefficients were also calculated for the case of fuel absorption and desorption. D was found to be 13.8×10^{-12} m^2/s for Sealant A, and 2.6×10^{-12} m^2/s for Sealant B. In the literature,[1] a value of 0.9×10^{-12} m^2/s was reported for immersion of a calcium dichromate-cured polysulphide sealant in aviation fuel (Avtur) at 25°C while, more recently,[3] the diffusion coefficients of a chromate-cured polysulfide sealant, and a silicone sealant in aviation fuel immersed at 25°C were found to be 1.39×10^{-12} m^2/s, and 13×10^{-12} m^2/s, respectively. In another publication,[24] it was found that the diffusion coefficient for a butadiene-acrylonitrile-epoxide sealant immersed in aviation fuel at 25°C was 1.5×10^{-12} m^2/s. Direct comparison of the findings in the present work and the literature values (Table II) is, of course, impossible, since both the chemistry of the materials and the nature of the diffusant is different. However, the order of magnitude of D found here compares well with the values found in the literature.

Combined water and fuel absorption

In an aircraft integral fuel tank, sealants are usually exposed at the same time to both the fuel stored in the tank, and to water which is present in the tank due to atmospheric condensation. The behavior of sealants exposed to a combined water and fuel environment was investigated by immersing samples of both sealants in water and jet fuel separately, and after a certain period of time moving the samples initially immersed in water into the fuel bath, and those initially immersed in fuel into the water bath. The immersion process took place at room temperature (23°C ± 2°C) and the results obtained are plotted in Figure 13. For the case of immersion in jet fuel following immersion in distilled water [Fig. 13(a)], Sealant A samples initially gained some more weight but after 4 h they started to lose weight. After a period of 1200 h, their net weight gain stabilized at 3.47%. In the case of immersion in distilled water following the immersion in jet fuel [Fig. 13(b)], apart from a small region at the beginning of the process where the weight of the samples showed a small increase followed by a small decrease, the weight gain did not show any significant deviation from the equilibrium level achieved during the initial immersion in fuel. The results obtained from tests on Sealant B were somewhat clearer. It was found that when immersed in fuel after water immersion the samples lost weight [Fig. 13(c)], but when immersed in water after fuel immersion they gained weight [Fig. 13(d)]. Taking into account that the distilled water and Type III jet fuel have very low mutual solubility as well as that Sealant B absorbs large amounts of water and significantly smaller amounts of fuel, the observed behavior could be explained by considering the concentration gradient that is introduced during the test. Therefore, when the water saturated samples were immersed in the fuel bath, there will be a concentra-

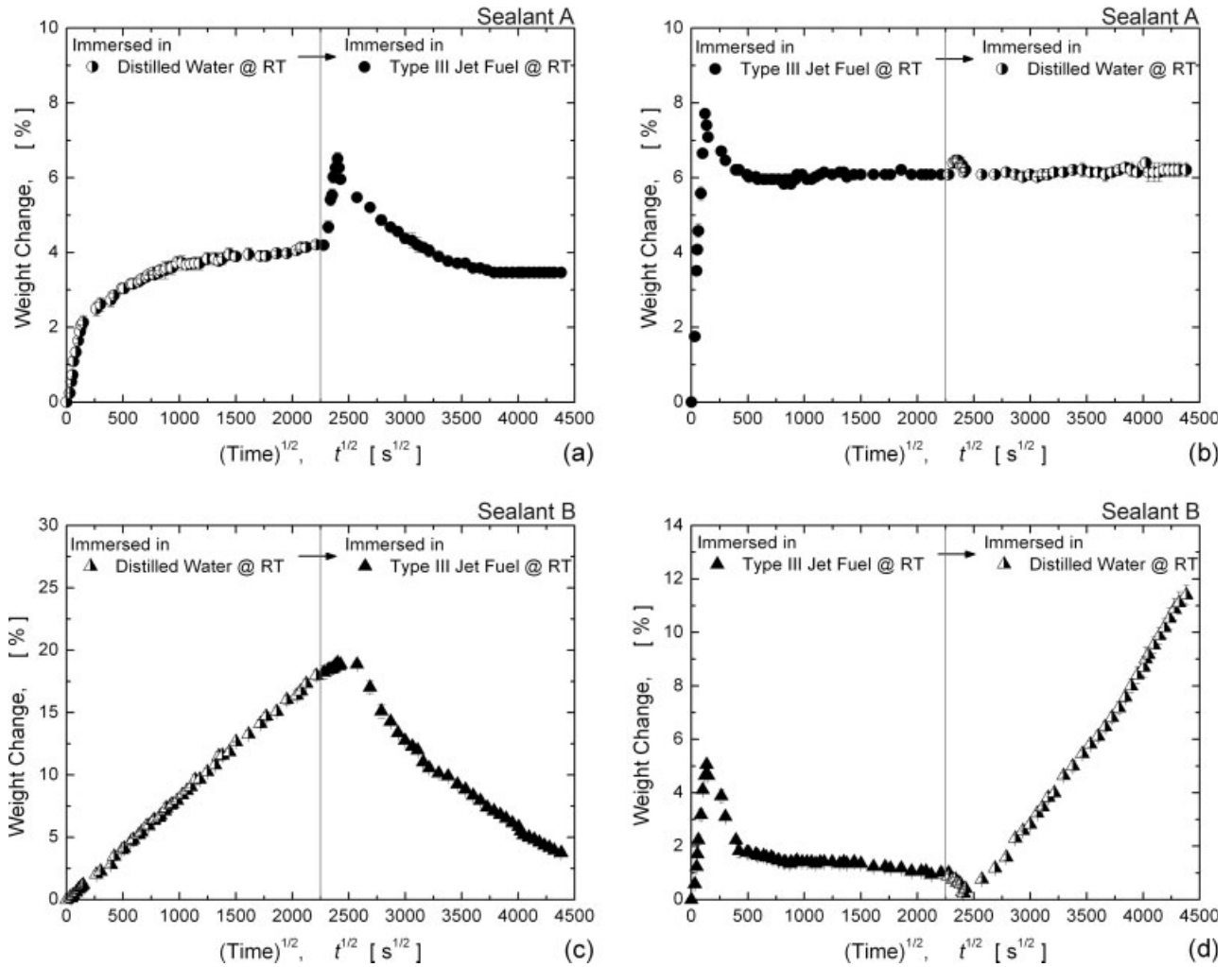

Figure 13 Percentage weight change data plotted with respect to the square root of time for both sealants during immersion in distilled water followed by immersion in jet fuel (a,c) and vice versa (b,d).

tion gradient that will drive water out of the samples and accordingly drive fuel in. Consequently, the overall weight will decrease until equilibrium is reached. The opposite will occur when fuel saturated samples are placed in the water baths.

RESULTS AND DISCUSSION OF GLASS TRANSITION TEMPERATURE TESTS

Glass transition temperature of dry Sealant A and Sealant B

Since both the base and the curing agent of Sealant A are polymeric, they should to have their own glass transition temperature. Evaluation of these T_gs was necessary to interpret the results for the cured sealant. In Figure 14, the variation of damping with respect to temperature is plotted for both the uncured base and the curing agent of Sealant A. The damping of the uncured Sealant A base material shows a clear and sharp peak, which provides a measured glass transition temperature of -62.2°C. There is also another very wide peak at a lower temperature (-105.3°C). This could either be a secondary β-transition of the polymeric material or it could be due to the melting of residual monomer in the polymer. Since polythioether-based sealants do not have bulky side groups attached to the backbone chain, they are unlikely to have β-transitions. However, the base material was produced by the reaction of a dithiol with a divinyl-ether[7] and it could be expected that the monomers will not be 100% reacted. Residual monomer will have a melting point, which could give rise to an apparent transition in the polymer. The melting point, for example, of ethenyloxyethene is -101°C.

On the other hand, the curing agent contains liquid epoxy resins that will have transition temperatures below room temperature. Two peaks appear in the damping curve of the curing agent at temperatures below zero, the first at -15.0°C and the second at -29.8°C. This indicates that the curing agent con-

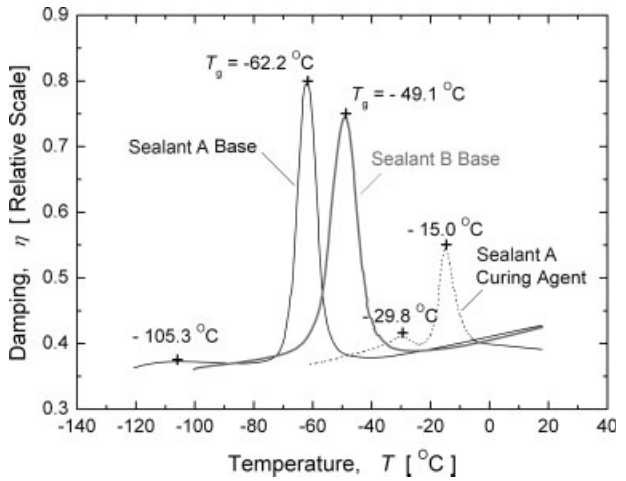

Figure 14 Variation of damping with respect to the temperature for Sealant A and Sealant B components (base and curing agent).

tains either two different epoxy resins with different molecular weights or one epoxy with two low temperature transitions. The peak at −29.8°C could possibly be the β-transition peak of the Bisphenol A resin, which was previously found to be in the same temperature range.[25]

The uncured base of Sealant B was also tested to evaluate its glass transition temperature. This was found to be −49.1°C from the damping curve (Fig. 14).The curing agent of this sealant is not polymeric (MnO_2), and it does not experience any glass transition.

Four different specimens were tested for the evaluation of the glass transition temperature of the dry, cured Sealant A material. In Figure 15(a) the resonance frequency and the damping of two beam specimens were plotted over a wide range of temperatures. The glass transition temperature evaluated from the frequency curves was found to be −55.4°C ± 1.0°C, while from the damping curve it was −52.4°C ± 1.0°C. These values are the average values from four specimens and they correspond to the T_g observed during the warming up stage. There was a 2°C difference between the values obtained from the frequency curve and those obtained from the damping, which is a result of the difference in the methods used to measure T_g. The dynamic behavior of the two specimens plotted in Figure 15(a) followed the same trend. Cured Sealant A shows, apart from the main glass transition temperature, another, low temperature transition, at −106.7°C ± 1.3°C, which is clearly observable on the damping curve. This low temperature transition is in the same temperature region where the low temperature transition of the uncured base material occurs. There are some deviations between the two dry specimens, possibly due to differences in the geometry and mass of the systems as well as the degree of cure. For example, the peak of the damping curve for specimen ABTG4 is higher than that of specimen ABTG1 and the glass transition temperature is also higher. Since both specimens were tested soon after the end of the curing process, this difference could be attributed to a slight variation in the degree of cure. Thus, a comparison between the two specimens, in terms of absolute frequency or damping values cannot be done. The only comparison that we could satisfactorily achieve is for the same specimen before and after immersion.

In Figure 16(a), the resonance frequency and damping curves of two specimens of Sealant B, prior to any kind of immersion are plotted. The glass transition temperature resulting from the resonance curves was −48.4°C ± 1.4°C, and from the damping curves was −44.9°C ± 1.1°C.

Glass transition temperature of Sealant A after water/fuel absorption and desorption

The glass transition temperature was also evaluated after immersion in distilled water at 50°C as well as after drying the immersed specimens and driving out any gained moisture. In Figure 15(b), the resonance frequency has been plotted over a wide range of temperatures for specimen ABTG1 after 1014 h in distilled water at 50°C. The percentage weight gain for this particular specimen was 4.20%. The measured resonance frequency varied slightly compared with that of the specimen prior to water immersion. In fact, the resonance frequency was found to be slightly lower at room temperature, which is probably due to the mass increase of the system. It was also found to be higher at very low temperatures, which can be due to the combination of volume swell of the sealant layer and, consequently, an increase in thickness, as well as a small increase in modulus. The glass transition temperature does not seem to change significantly with the presence of water, since it was measured to be close to that obtained for dry samples. In addition, it is worth noting the overall behavior of the material over this wide range of temperatures. Apart from the main transition, there were some other transition-like anomalies observed. The first one was in the temperature range from −70 to −60°C, while the other one was in the range from −25°C to −5°C. These transition-like anomalies appear in the same temperature ranges where the uncured base and curing agent have their own transitions. Therefore, some unreacted base and/or curing agent might be being mobilized by the presence of water. The T_g of specimen ABTG1 evaluated from the damping curve, as shown in Figure 15(b), was also very close to the average value of the dry specimens. There is also a

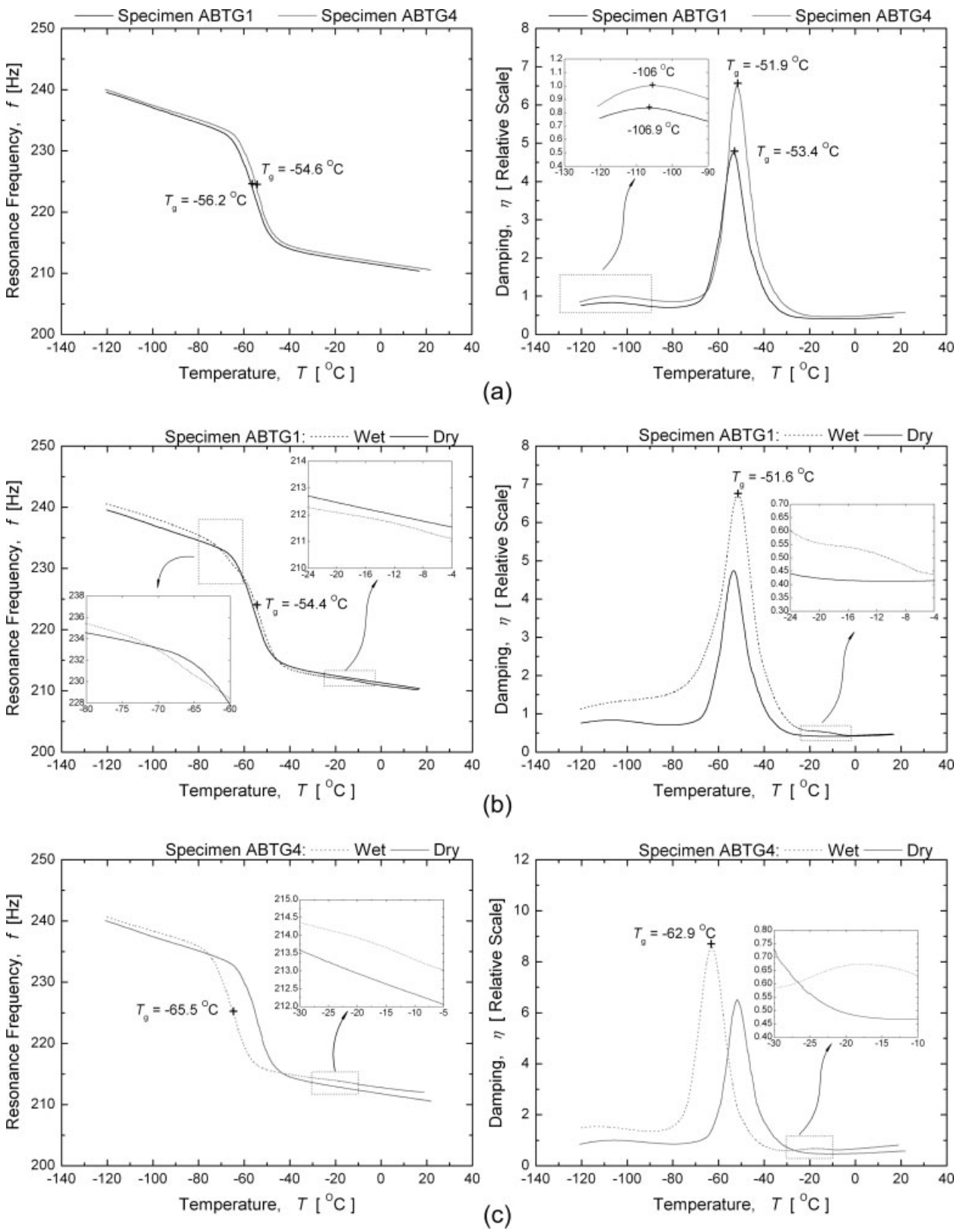

Figure 15 Variation of resonance frequency and damping with respect to the temperature for Sealant A specimens (a) dry, (b) after water immersion, and (c) after fuel immersion.

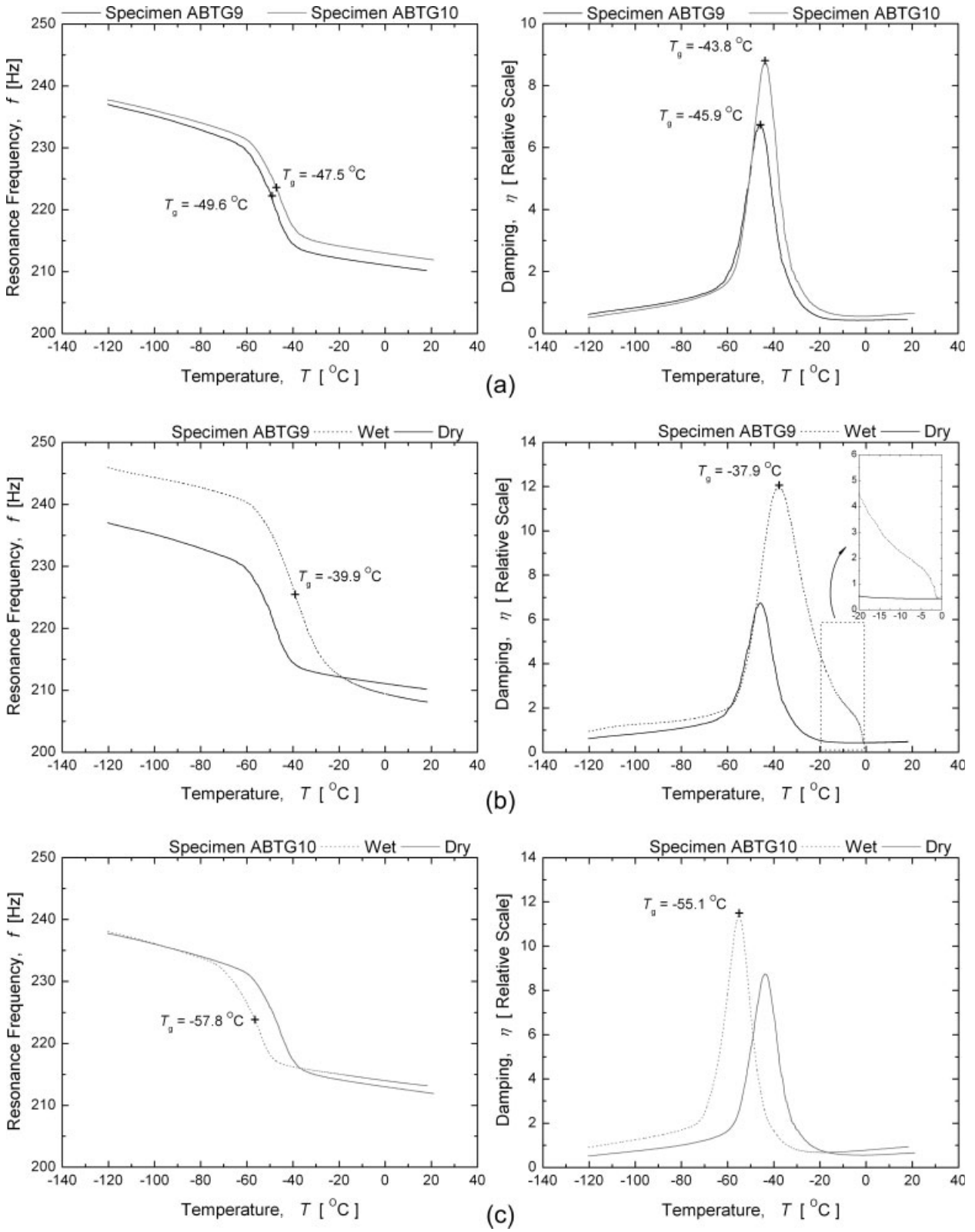

Figure 16 Variation of resonance frequency and damping with respect to the temperature for Sealant B specimens (a) dry, (b) after water immersion, and (c) after fuel immersion.

TABLE III
Average Measured Values of the Glass Transition Temperatures for Sealant A and Sealant B

	T_g (°C)			
	Warming stage		Cooling stage	
Test/weight change (%)	Damping	Frequency	Damping	Frequency
Sealant A				
D/0	−52.4 ± 1.0	−55.4 ± 1.0	−53.0 ± 1.3	−55.6 ± 1.5
W/4.2	−52.0 ± 0.5	−55.0 ± 0.9	−52.9 ± 0.3	−56.9 ± 0.5
F/5.6	−62.5 ± 0.6	−65.2 ± 0.4	−61.4 ± 0.7	−62.9 ± 0.9
DW/−1.9	−51.7 ± 0.6	−54.9 ± 0.8	−51.8 ± 0.8	−54.6 ± 0.8
DF/−3.3	−53.4 ± 0.1	−57.4 ± 0.1	−51.8 ± 0.1	−57.5 ± 0.1
Sealant B				
D/0	−44.9 ± 1.1	−48.4 ± 1.4	−44.5 ± 1.1	−47.8 ± 1.2
W/27.9	−40.2 ± 0.1	−41.3 ± 0.1	−40.8 ± 0.1	−42.4 ± 0.1
W/49.0	−37.9 ± 0.1	−39.9 ± 0.1	−37.4 ± 0.1	−38.6 ± 0.1
F/1.9	−55.0 ± 0.1	−57.6 ± 0.3	−55.1 ± 0.3	−57.1 ± 0.3
DW/1.6	−43.8 ± 0.2	−46.7 ± 1.0	−44.3 ± 0.7	−46.3 ± 0.2
DF/−6.1	−45.1 ± 0.8	−48.7 ± 0.4	−45.2 ± 0.1	−48.3 ± 1.0

D, dry samples; W, after water immersion; F, after fuel immersion; DW, dried after water immersion; DF, dried after fuel immersion.

damping variation in the temperature range from −25°C to −5°C. The damping value at T_g increased after water immersion and the area under the damping curve was found to be 66% higher. After drying the specimens and reevaluating T_g, it was found that, on the basis of the damping curve, it was equal to −51.7°C ± 0.6°C, while from the resonance curve it was −54.9°C ± 0.8°C. Hence, no significant difference could be observed between the dry and the saturated and dried specimens.

Unlike the samples immersed in water, those that were immersed in fuel have shown a significant change in their glass transition temperature. In Figure 15(c), the resonance frequency for the ABTG4 specimen after fuel immersion is plotted with respect to temperature. The T_g was found to be 10°C lower compared with the average value of the dry specimens. A noticeable shoulder could also be seen in the resonance curve in the temperature range from −25°C to −5°C. In the damping curve a shoulder appears in the same temperature range as in the resonance curve. The specimens saturated with fuel show a higher damping value at T_g and a 38% increase in the total area under the damping curve. After drying these specimens in air at room temperature for nearly 500 h, the glass transition temperature values returned close to the values of the initial dry specimens before any water or fuel immersion. All average T_g values as calculated from both the warming and cooling stages of the tests are listed in Table III.

Glass transition temperature of Sealant B after water/fuel absorption and desorption

After ~1200 h of immersion in distilled water at 50°C, specimen ABTG9 was tested to evaluate the glass transition temperature. The weight gain of the specimen was measured as 49.0%. Both the monitored resonance frequency and damping are plotted in Figure 16(b) with respect to temperature. The change in T_g was significant and from the resonance curve it was found to be −39.9°C ± 0.1°C, an 8.5°C increase, while from the damping curve it was found to be −37.9°C ± 0.1°C, which corresponds to a 7°C increase. Exactly the same trend was found for a specimen having a lower weight gain after immersion (Table III). This observation is against traditional theories, which predict a glass transition temperature reduction once the polymeric material is saturated with water. The overall damping of the specimen increased nearly two times with the area under the damping curve increasing by 115%. Another interesting finding was that the damping of the specimen showed a very rapid change in the vicinity of 0°C. This observation was made for all the specimens tested during the warming up stage. Although the variation of damping was monitored during the cooling stage, it was very difficult to identify any other transitions apart from the main ones, since the cooling rate was much faster than the warming rate and the data capture was relatively slow. The resonance frequency at room temperature of the beam specimen decreased with respect to the frequency of the same beam before water immersion. Because the sealant material absorbs water, three things happen. First, the mass of the beam increases; second, the thickness of the sealant layer increases; and third, the stiffness of the sealant layer decreases. These changes generally lead to a decrease of the resonance frequency. At very low temperatures, it was found that the resonance frequency increases significantly in comparison to the same specimen

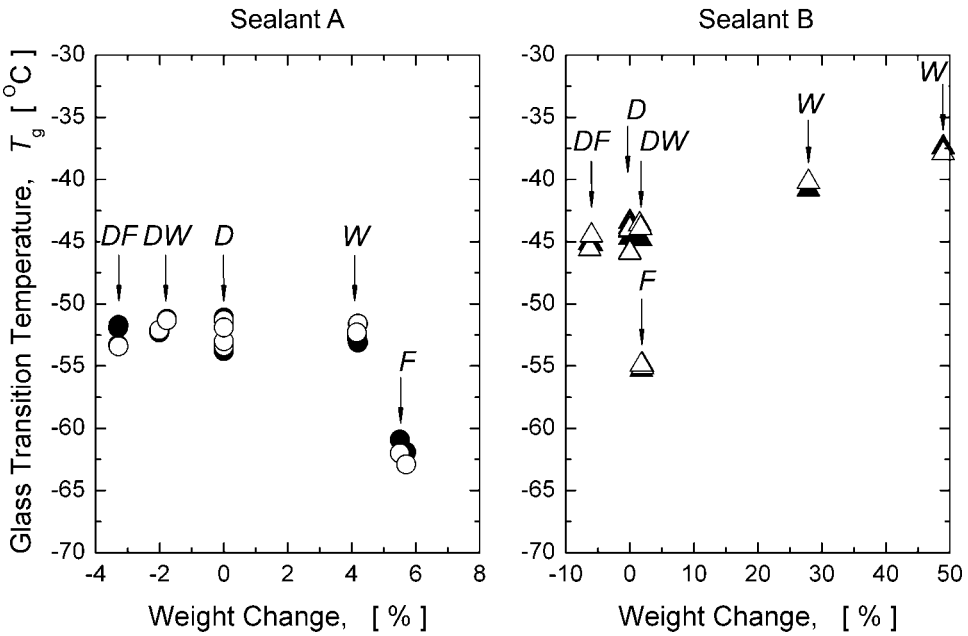

Figure 17 T_g plotted as a function of the percentage weight change for both sealants (D, dry samples; W, after water immersion; F, after fuel immersion; DW, dried after water immersion; DF, dried after fuel immersion; results obtained from: ○ warming stage and ● cooling stage).

before water immersion. More precisely, the resonance frequency at −120°C was found to be 245.92 Hz compared to 237.02 Hz before immersion. Such a big change indicates that the stiffness of the material at this specific temperature has increased significantly. Both the anomalous behavior of the damping of the system around 0°C and the much higher effective stiffness of the wet samples at very low temperatures point toward the existence of water droplets in the bulk of the sealant that form as ice below 0°C. This was already predicted by the DSC tests presented earlier. Therefore, the water droplet formation can also be implied from measurements of the damping in water saturated samples. After removing nearly all the water adsorbed by drying the specimens, T_g decreased to the values measured on the specimens before any kind of immersion (Table III).

The effect of fuel immersion seems to be the opposite to water for this sealant. Figure 16(c) shows the variation in frequency and damping of a specimen that had been immersed in fuel for ~ 650 h. T_g was depressed by 10.5°C as measured from both damping and frequency. The resonance frequency did not change significantly, while the damping peak value increased as well as the area under the curve by 28%. The drying process seemed to have the same effect as for all the other cases and drove the T_g back toward the value of the unconditioned materials. In other words, the shift of the glass transition temperature due to the presence of fuel appears to be a reversible process.

Discussion of T_g results

In Figure 17, the measured values of the glass transition temperature obtained from the damping curves for Sealant A and Sealant B, respectively, are plotted as a function of weight gain for all the ageing processes. Since the T_g values obtained from the frequency have shown the same trend, it was thought unnecessary to plot them too. The legend of the graph explains which letter corresponds to which process. First of all, examining Figure 17, it should be noted that there were no significant differences in the values measured from the cooling or warming stages. The same can be concluded by considering the average T_g values in Table III.

An important finding is that there was no apparent effect on the measured value of the glass transition temperature of Sealant A after exposing the specimens in distilled water. It is not clear in what form the water is present in Sealant A. No evidence of water droplet formation was found in the previous section. It is unlikely that the amount of water absorbed at the conditions examined here could cause plasticization of the material since there was no observable depression of T_g.

On the other hand, there was a significant effect when samples were immersed in fuel. Fuel immersion drives the T_g to much lower values. This depression of the glass transition temperature appears to be a reversible process, since it was found that, after drying the specimens and consequently

removing any fuel, the T_g values were returned to be close to the values of the initially dry specimens. This would suggest that the reduction in glass transition temperature is due to plasticization of the sealant by the fuel. Therefore, fuel diffuses into the sealant and breaks the existing interchain Van der Waals forces resulting in an increase in molecular chain mobility.

Like Sealant A, the values obtained for T_g were plotted against the weight gain of the specimens for Sealant B (Fig. 17). It can be seen that there is a clear increase in the glass transition temperature with increasing weight gain when immersed in distilled water, and an obvious decrease when immersed in fuel. As for Sealant A, the glass transition temperature shifts back to the initial value when the water or fuel are removed from the specimen by drying. The depression of T_g after fuel immersion indicates plasticization of the material due to the presence of the fuel. It is possible that similar processes as for Sealant A are occurring when synthetic fuel diffuses into Sealant B. However, the change of T_g for the water immersed samples appears to be more complex and indicates possible antiplasticization effects. The fact that, after desorption, T_g shifts back to the value obtained for the dry specimens implies that the antiplasticization effect is purely due to the presence of water.

A possible explanation of the observed antiplasticization effect of water onto Sealant B and the overall unusual behavior could be given based on physical and chemical considerations. It was found in the previous section that Sealant B absorbs large amounts of water. Moreover, the absorbed water forms droplets of solution which form ice particles in the bulk of the material when the temperature is decreased below the freezing point of water. These ice particles, whose existence is implied by the DSC experimental results, are likely to act as macroscopic fillers in the sealant (Fig. 18). In such a case, the stiffness of the material (sealant with randomly dispersed ice particles in its volume) would significantly increase compared to sealant that was not subjected to water immersion. That is clearly indicated by the results at very low temperatures of the measured resonance frequency, which is proportional to the stiffness of the tested material [Fig. 16(b)]. Payne and Whittaker[26] claimed that the addition of fine particulate fillers to amorphous rubbers increased their modulus.

As for the antiplasticization effect and the increase in T_g, it is possible that some interactions will develop between the macroscopic water droplets and the sealant network. It should be noted that the water is a very polar liquid, as is the backbone of the polysulphide sealant, because of the existence of oxygen (O). Therefore, it is likely that polar interactions between the water and the polymer backbone would exist. This could also lead to hydrogen bonding and the creation

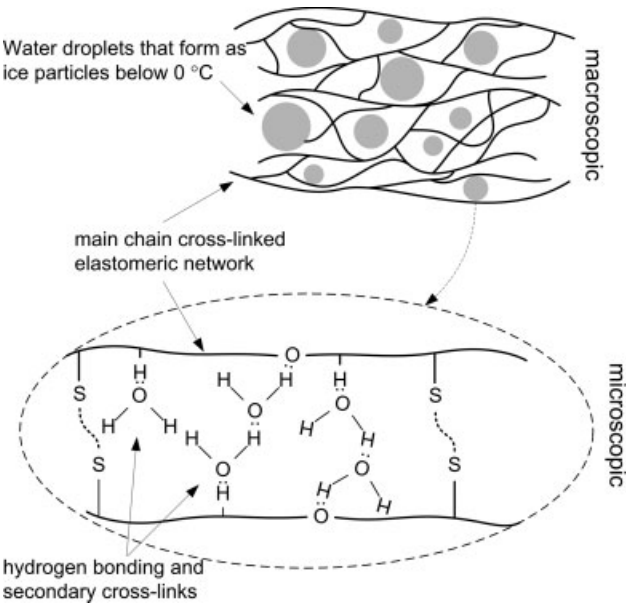

Figure 18 Physical and chemical interactions between the water droplets that form as ice particles below 0°C and the molecular network of Sealant B at macroscopic and microscopic level.

of secondary crosslink networks that would further restrict the molecular motion (Fig. 18). Zhou and Lucas[27] who investigated the hygrothermal effects in epoxy resins postulated that the effect of secondary formed crosslinks on T_g is relatively weak. However, the amount of water absorbed by Sealant B is much higher than that absorbed by their epoxies ($\sim$ 8% by weight), and therefore it is possible that the density of the formed secondary networks could be much higher. Such an argument seems reasonable to explain the measured increase in T_g. It can also be recalled from the literature that Petrovic et al.[28] who incorporated micro-silica and nano-silica particles into a single phase polyurethane elastomer, found that the T_g obtained from DSC measurements did not display a strong dependence on the filler content, but DMA measurements on the same materials indicated a 10°C increase (−49°C to −39°C) for both materials. This phenomenon was credited to chemical and physical interactions between the filler and the polyurethane. Thus, it is possible that the presence of fillers and their chemical interactions with the polymer network can cause an increase in the measured T_g. Finally, it should be noted that these interactions are reversible as suggested by the measured T_g values after drying the saturated samples.

However, the action of water as an antiplasticizer was not confirmed by Gick[1] who investigated the effect on the glass transition temperature of the water absorption by a polysulphide sealant cured using calcium dichromate ($CaCr_2O_7$). The DSC tests performed during that research on samples with a 120% by weight

water gain gave no detectable shift of T_g. The explanation given was that no shift occurred because T_g is too far below the freezing point of water. However, two years earlier, Hinkley and Holmes[29] performed tests by immersing three different polychloroprene rubber compounds in salt and fresh water, and attempted to see whether plasticization was occurring using DSC measurements. In every case, the samples which had been saturated showed glass transition temperatures 3–5°C higher than the corresponding dry material. They hypothesized that the water or salt solution extracted certain compounding ingredients or by-products, resulting in this increase. However, they did not test their samples after drying to examine whether this increase in the glass transition temperature was reversible or not, which is the case in the tests presented here. A similar explanation, where the leached compounds may act as plasticizers in the dry specimens, was recently given in the literature[30] for the clear antiplasticization effect observed on glass fiber reinforced composite-polyester and vinyl ester laminates after immersion in distilled water at 30°C and at 60°C.

CONCLUSIONS

The main findings and conclusions from this study may be summarized as follows:

1. Sealant A (epoxy-cured polythioether sealant) absorbs small amounts of water (~ 6.2%) and the diffusion process can be regarded as Fickian. Fuel absorption levels are slightly higher (~ 8.6%) and the weight gain curve is characterized by an early maximum followed by a decrease until equilibrium is reached.
2. The glass transition temperature of Sealant A was found to be unaffected by the presence of water but strongly affected by the presence of fuel. A drop of the order of 10°C was measured in the latter case. The plasticization behavior of Sealant A when immersed in jet fuel can be explained by the free volume theory.
3. Sealant B (MnO_2-cured polysulphide sealant) is characterized by a large water uptake and a strong affect of the immersion temperature. The observed behavior is clearly non-Fickian and it was attributed to water droplet formation in the sealant because of the existence of hydrophilic impurities that act as sinks for the water diffusing into the material. When immersed in jet fuel, Sealant B showed very similar behavior to that of Sealant A with the weight gain curve demonstrating an early maximum followed by a decrease until equilibrium was reached.
4. The glass transition temperature of Sealant B increased after exposure in distilled water. This antiplasticization effect was attributed to interactions between the sealant polymeric network and the water droplets that form as ice at temperatures below 0°C. The high polarity of the diffusant (H_2O) and that of the polymer backbone could possibly lead to the formation of hydrogen bonds and secondary crosslink networks. Fuel acts as plasticizer for the sealant, depressing the glass transition temperature by 10°C.
5. The variation of the glass transition temperature after water and fuel exposure was found to be a reversible process for both sealants.

References

1. Gick, M. M. S. Ph.D. Thesis, Polytechnic of North London, 1988.
2. Ong, C.-L.; Shu, W.-Y.; Shen, S. B. Int J Adhes Adhes 1992, 12, 79.
3. Comyn, J.; Day, J.; Shaw, S. J. Int J Adhes Adhes 1997, 17, 213.
4. Brewis, D. M. In Durability of Structural Adhesives; Kinloch, A. J., Ed.; Applied Science Publishers: London, 1983.
5. Adams, R. D.; Comyn, J.; Wake, W. C. Structural Adhesive Joints in Engineering; Chapman & Hall: London, 1997.
6. Comyn, J. In Adhesive Bonding: Science, Technology and Applications; Adams, R. D., Ed.; Woodhead Publishing: Cambridge, 2005.
7. Clark, L. J.; Cosman, M. A. Int J Adhes Adhes 2003, 23, 343.
8. Lowe, G. B. Int J Adhes Adhes 1997, 17, 345.
9. Usmani, M. Polym-Plast Technol Eng 1982, 19, 165.
10. NF T 76-142. Méthode de préparation de plaques d'adhésifs structuraux pour la réalisation d'éprouvettes d'essai de caractérisation, 1988.
11. Da Silva, L. F. M. Ph.D. Thesis, University of Bristol, 2004.
12. ISO 1817. Rubber Vulcanized-Determination of the Effect of Liquids, 1999.
13. Guild, F. J.; Adams, R. D. J Phys E: Sci Instrum 1981, 14, 355.
14. Singh, M. M. Ph.D. Thesis, University of Bristol, 1993.
15. Crank, J. The Mathematics of Diffusion; Clarendon Press: Oxford, 1975.
16. Fujita, H. Adv Polym Sci 1961, 3, 1.
17. Usmani, M.; Chartoff, R. P.; Warner, W. M.; Butler, J. M.; Salyer, I. O.; Miller, D. E. Rubber Chem Technol 1981, 54, 1081.
18. Loh, W. K.; Crocombe, A. D.; Abdel Wahab, M. M.; Ashcroft, I. A. Int J Adhes Adhes 2005, 25, 1.
19. Thomas, G.; Muniandy, K. Polymer 1987, 28, 408.
20. Briggs, G. J.; Edwards, D. C.; Storey, E. B. Rubber Chem Technol 1963, 36, 621.
21. Hanhela, P. J.; Huang, R. H. E.; Brenton, P. D. Indus Eng Chem: Product Res Dev 1986, 25, 321.
22. Hanhela, P. J.; Huang, R. H. E.; Brenton, P. D.; Symes, T. E. F. J Appl Polym Sci 1986, 32, 6415.
23. Lowe, G. B.; Lee, T. C. P.; Comyn, J.; Huddersman, K. Int J Adhes Adhes 1994, 14, 85.
24. Comyn, J.; Day, J.; Shaw, S. J. Int J Adhes Adhes 2000, 20, 77.
25. Mangion, M. B. M.; Johari, G. P. J Polym Sci Part B: Polym Phys 1990, 28, 71.
26. Payne, R.; Whittaker, R. E. J Appl Polym Sci 1941 1971, 15.
27. Zhou, J.; Lucas, J. P. Polymer 1999, 40, 5513.
28. Petrovic, Z. S.; Javni, I.; Waddon, A.; Banhegyi, G. J Appl Polym Sci 2000, 76, 133.
29. Hinkley, J. A.; Holmes, B. S. J Appl Polym Sci 1986, 32, 4873.
30. Boinard, E.; Pethrik, R. A.; Dalzel-Job, J.; MacFarlane, C. J. J Mater Sci 1931 2000, 35.